EXPERIMENTAL ASSESSMENT OF AN ACTIVE FLAP DEVICE

Philippe Leconte
Research Unit Head
ONERA, Châtillon, France
Philippe.Leconte@onera.fr

Hugues Mercier des Rochettes
Research Engineer
ONERA, Lille, France
hmdr@imf-lille.fr

ABSTRACT: A project called RPA (Rotor à Pales Actives) was launched three years ago to study the possible benefits of implementing active trailing edge flaps on a helicopter main rotor. The main objectives of this project are to decrease BVI noise in descent flight and improve the dynamic behavior of the rotor throughout the largest possible flight domain. After a first phase dedicated to the design of the best flap configuration at scale 1, the second phase of the project deals with the design of a wind-tunnel scale model of a rotor equipped with active flaps. An off-the-shelf piezo-electric actuator is used together with a specific patented flap-driving mechanism. Such an active device was tested under centrifugal loads as well as under aerodynamic loads in order to prepare future wind-tunnel tests. The results obtained under centrifugal loads allowed to clear the active device but the aerodynamic testing showed that some improvements were needed. Corresponding modifications are under way to fully clear the active device to be used on a complete rotor model.

INTRODUCTION

When the blades of the main rotor of a helicopter perform a revolution, they encounter extremely varying aerodynamic conditions, coming from the combination of rotor speed and helicopter forward speed, which can result in high vibration loads transmitted to the fuselage. Beside this, the inherent aerodynamic flow around a blade generates a tip vortex which is convected downward inside the rotor wake, along a helicoïdal path. During certain flight configurations, such as descent, the combination of the descent rate of the aircraft and the convection of the wake may cause the vortices to impact on some of the other blades, creating BVI (Blade-Vortex-Interaction) noise. During the past thirty years, noticeable consideration has been devoted to the improvement of rotary-wing vehicles, notably with respect to noise and vibrations. As such, the main rotor of helicopters, and more precisely the blades themselves have been the subject of numerous optimization studies. Passive means [1 to 6] have been at first considered such as advanced planforms, sophisticated spanwise distribution of airfoils, refined twist laws, innovative blade tips, advanced structural designs.

Subsequently, other approaches such as HHC (Higher Harmonic Control) or IBC (Individual Blade Control) have been also successfully tested, although none of these could achieve the level of being used on commercial helicopters [7]. More recently, due to significant progress in the field of smart materials, innovative concepts such as active flaps or active twist started being studied.

Within the frame of the RPA (Rotor à Pales Actives) project launched three years ago at ONERA, numerical simulations allowed in a first phase to determine an optimal flap configuration to decrease both BVI noise and vibrations. The second phase of the project, now being dealt with, consists in designing, manufacturing, testing and analyzing a wind-tunnel scale rotor model with active flaps to validate numerical predictions. Therefore, an active system featuring both a flap and an actuator was designed. The tests of a complete rotor with flaps are a real challenge and preliminary tests were deemed necessary, more precisely related to the actual behavior of the active system under centrifugal and aerodynamic loads. Consequently, several tests in both laboratory and wind tunnel were performed to qualify the active system for future rotor model tests. Satisfactory behavior under centrifugal loads could be noticed, but some improvements, being tackled at the present moment, were dictated by the results of aerodynamic evaluation.

Presented at the American Helicopter Society 58th Annual Forum, Montréal, Canada, June 11-13, 2002.

THE RPA PROJECT

The RPA project aims to evaluate the benefits of active trailing edge flaps mounted on the blades of the main rotor of a helicopter. This project is carried out in close co-operation with DLR, Eurocopter and Eurocopter Deutschland.

Two main objectives drive the study, which are the reduction of BVI noise during descent flight and the reduction of vibrations [8,9] throughout the whole flight domain. Additional benefits in terms of aerodynamic performance are also addressed. Two flap concepts, respectively referred to as servo-flap and direct-lift flap, were at first considered. The former used a small chord flap, relying on the influence of aerodynamic pitching moment to induce blade torsion. The latter was based on large chord flap acting on the lift distribution. The span of the flap as well as its spanwise location was some of the parameters addressed during numerical simulations of a full-scale medium-class helicopter rotor. Optimal flap deflection laws were designed with respect to the objectives mentioned above for each flap configuration.

The small chord flap was finally chosen, and three possible spanwise locations were retained to be experimentally checked, depending on the contribution of the flap to decrease noise or vibration. Figure 1 shows the BVI noise reductions, calculated with ONERA aero-acoustic numerical codes, that can be expected for these three locations, illustrated on figure 2. As far as vibrations are concerned, gains of up to 90% on the 4-per-rev vertical force or 45% on the 3-per-rev in-plane moment in the rotating frame (inducing pitch and roll movements), without penalty on other unsteady forces, could be numerically obtained. During performance evaluation, gains were estimated as marginal.

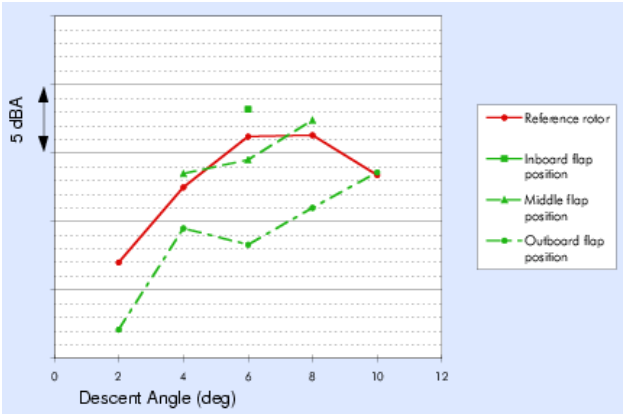

Figure 1 – Calculated BVI noise level

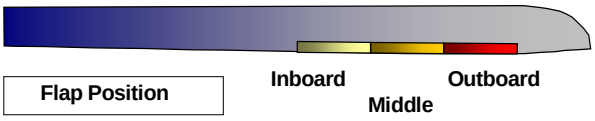

Figure 2 – Spanwise flap positions

Some of the physical phenomena, which contribute to noise alleviation, need to be experimentally demonstrated, such as the combination of blade tip vortex and flap tip vortex. Therefore, a four-bladed rotor model will be manufactured and tested in both S1MA (high speed for vibration) and DNW (low speed for noise) wind tunnels in order to validate the numerical simulations.

WIND-TUNNEL SCALE ROTOR

The external geometry of the wind-tunnel scale blade matches almost perfectly that of the full-scale blade, illustrated on figure 2, which is to be flight-tested by Eurocopter Deutschland and called ATR-a [10]. The only modification consists in using the same airfoil, OA312, all along the flapped area (70 to 90% of blade radius) to ease the numerical validation.

Another difference lies in the fact that an articulated hub will be used in the wind tunnel, whereas the full-scale hub is of HMR type.

The overall diameter of the Mach-scaled rotor is 4.2 m, the maximum blade chord being 140 mm. With respect to the calculations of the full-scale rotor, the flap dimensions at wind-tunnel scale are 210 mm in span and 21 mm in chord.

The internal structure of the wind-tunnel blade is classical and uses a main spar and a trailing edge spar made of uni-directional glass fibers. Carbon plies are used to manufacture the blade skins and foam is used to fill the inner space. Balancing weights made of Inermet are located in the leading edge area.

A specific structure made of carbon uni-directional fibers is implemented to accommodate the active flap system, i.e. actuator, driving mechanism, hinge system and flap.

Due to the higher value of the active system mass over total blade mass at wind-tunnel scale, dynamic similarity with full scale cannot be fulfilled.

ACTUATION METHODS

Requirements

From the specifications released by industry for the full-scale active system and considering a geometrical reduction factor of 2.619, the following requirements had to be satisfied by the active device for the Mach-scaled rotor :

- natural frequency of the flap/hinge axis : 393 Hz theoretical but 150 to 200 Hz was estimated adequate ;
- minimal flap deflection : ± 5°, 78 Hz, static moment of 1.22 Nm for hinge centered at 0% ;
- ideal flap deflection : ± 15°, 262 Hz, static moment of 4.91 Nm for hinge centered at 0% ;
- flap actuation frequencies ranging from 0 to 5-per-rev with respect to rotor rotation speed ;
- required energy/kg of actuators : max of E/m = 0.15 to 0.3 Joule/kg
- maximum centrifugal field : 2300 g.

All these specifications for blade model show the stringent need of an active device able to fit inside a limited volume with a high natural frequency and operating with high flap angular deviations under high hinge moments and high centrifugal field.

Overview of actuation solutions

A large array of technical solutions to actuate the flaps was considered during the design phase : pressurized air, hydraulics, electric motors, and various smart materials configurations. The specifications, notably in terms of actuation frequencies and due to the requirement of operating in the rotating system, led to the selection of a solution based on smart materials. Existing commercial actuators, such as those proposed by a French company named CEDRAT RECHERCHE, as well as recently developed prototypes such as that of University of Maryland [11] were looked at. Table 1 presents a comparison of the performance of such devices.

Table 1 - Comparison of capabilities of smart actuators

	Maryland 1/7th scale blade model *in-house fabricated*	Maryland full scale blade *Prototype*	CEDRAT APA200M *mass production*	CEDRAT APA500L *mass production*	CEDRAT APA230 For 1/ 2.62th model *mass production*
Actuator technology	Multi-layer actuator configuration (8 layers)	Piezostacks with L-L amplification mechanism	Piezostacks in elliptic housing	Piezostacks in elliptic housing	Piezostacks in elliptic housing
Voltage	± 134V → ± 400 V	0-120 V	0- 200 V	0- 200 V	0- 200 V
Mass of actuator	14 g	634 g	16.4 g	208 g	250 g
Blocked force (F)	8 N	53 N(20 N*)	56 N	570 N	800 N
Maximum stroke (x)	165 µ	2540 µ (889 µ*)	200 µ	500 µ	230 µ
Stiffness	$0.048\ 10^6$ N/m	$0.021\ 10^6$ N/m	$0.280\ 10^6$ N/m	$1.140\ 10^6$ N/m	$3.48\ 10^6$ N/m
Resonance frequency	above 150 Hz	Above 150 Hz	800 Hz	450 Hz	800 Hz
Energy to weight ratio of actuator	$23.6\ 10^{-3}$ Nm/kg	$53.1\ 10^{-3}$ Nm/kg ($28\ 10^{-3}$ Nm/kg*)	$170.7\ 10^{-3}$ Nm/kg	$342.5\ 10^{-3}$ Nm/kg	$184.0\ 10^{-3}$ Nm/kg
Ratio of Energy.. /L-L Energy..	0.44	1	3.21	6.45	3.47
Width (chord axis)	33 mm	71 mm	17 mm	55 mm	69 mm
Length (span axis)	60 mm	183 mm	55 mm	145 mm	140 mm
Thickness	2 mm to 5 mm	19 mm	5 mm	10 mm	10 mm
Peak-to-peak flap deflection	±11°.5	±11°.5	±4°.5 (extrapolated)	±9°.5 (extrapolated)	±4°.5

** test with spring applied on actuator*

One another commercial possibility could have been the actuator developed at MIT, known as X-frame. However, no detailed data could be obtained about that design.

Although the respective scales of University of Maryland and ONERA blade models are not directly comparable, the energy to weight ratio clearly shows that the CEDRAT solution yields significantly better results.

As a result, an actuator from the CEDRAT Company was selected.

APA ACTUATOR

Principle of operation

As mentioned above, the elected actuator for a first prototype was an off-the-shelf APA230 type, manufactured by CEDRAT, slightly modified for the present application. Four stacks made up of soft piezoelectric ceramic are located and pre-stressed on the major axis of an elliptic steel frame. When a positive voltage is applied to the stack, its length increases and the minor axis of the elliptic frame decreases with a stroke ratio of about 2.6.

The power amplifier used to supply the actuator is a Bop200-1M made by KEPCO limited to ± 200V and ± 1 A current.

Some of the main characteristics of the CEDRAT APA 230 actuator are presented in Table 1.

Flap device description

THE APA actuator is clamped on a surrounding rectangular frame on one side and is supported by a centrifugal blade on the other side to withstand the torque generated by the overhang under centrifugal field (see figure 3). The frame is closed in operation by two external plates to stiffen the whole system.

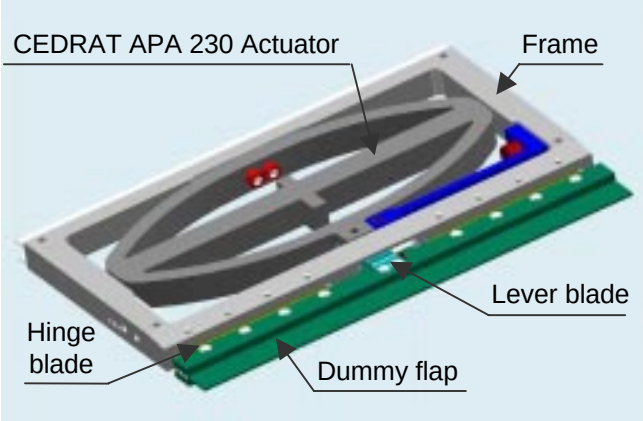

Figure 3 - 3D view of the active flap system

The elliptic actuator deflects the flap by means of a lever blade. The flap can rotate around a pseudo-axis given by the flexion deformation of two composite hinge blades. These blades are located on each side of the lever blade and clamped both in the flap and in the frame (see figure 3). A patent for such a configuration has been applied for by ONERA. The magnitude of the flap deflection can be adapted by changing the radius of the connection point of the lever blade on the flap. At rest, i.e. without power supplied to the actuator, the flap lies in the maximum downward deflection.

The main advantages and drawbacks of the active system can be listed as follows :

Advantages :

- no friction : calculations including the radial and centrifugal loads with 4 smooth bearings give a friction moment between 29 and 47% of the actuator maximum moment. With thrust bearings, these values can be decreased between 8 and 12% but there is no room for such a kind of bearings ;
- no local wear since kinematics is ensured by elastic deformation ;
- no mechanical play. Since the stroke of the actuator is rather small, not the slightest part of it should be wasted. Furthermore, the transfer function between the actuator and the flap must be as limited as possible to enable an easy control of the flap ;
- the centrifugal force initiated by the flap mass is withstood by the hinge blades along the full span of the flap ;
- presumed good fatigue behavior as preliminary calculations on the hinge blades (two layers at 0°) give an α fatigue margin of 1.27 ;
- simplicity of assembling, no maintenance ;
- in case of cracks developing on lever blade and long hinge blades, these would be visually easily detected ;
- high natural frequencies estimated between 100 and 200 Hz according to the type of setting ;
- the hinge blade can act as an aerodynamic sealing between upper and lower surfaces of the blade ;

Drawbacks :

- due to the use of the hinge blades, the equivalent rotation axis slightly moves fore and aft during the flap deflection. This could be overcome thanks to the use of a pseudo-ball joint on each of the flap tips ;
- for similar reasons, the accurate flap angular position measurement is not easy ;
- the connecting device between the actuator and the flap can be seen as a reversible system (depending on its intrinsic stiffness).

Instrumentation

Two different approaches were considered to accurately measure the flap deflection angle, respectively using strain gauge bridges and Hall effect sensors.

In the case of strain gauges, two locations could be foreseen : on the lever blade connecting the actuator to the flap or on the composite flap hinges. The former solution, adopted on the initial prototype, provides ample space to install the gauges but the latter are submitted to high fatigue level. Furthermore, the signal measured with these gauges would not include the contribution of the softness of the hinge blades. So, the most favorable location would be to glue the gauges on the hinge blades and this solution will be tested in a near future. A smart cabling, along with suitable data acquisition could also allow to estimate the spanwise flap torsion in operation.

When using Hall effect sensors, the magnets are glued at the flap tip and the sensors located in the blade trailing edge. Attention has to be paid to the influence of centrifugal load, since any change, even minor, in the gap between magnet and sensor results in significant calibration deviation.

Associated with the flap angle measurement presented above, a strain gauge bridge implemented on the elliptic frame of the piezo actuator allows measuring its stroke.

INTEGRATION STEPS

The design of the wind-tunnel scale flap-equipped blade was in fact started in parallel with the numerical simulations of the full-scale concept due to the challenge it was estimated to be. Beside this, as the operating costs of both S1MA and DNW wind tunnels represent a significant amount of money, it was stated as necessary to demonstrate the feasibility and the reliability of an active flap system prior to test it on a complete rotor. Therefore, preliminary tests were decided to separately assess the behavior of the active device under respectively centrifugal and aerodynamic loads.

CENTRIFUGAL TESTS

Test model

A specific model was designed and built to test the capability of the APA230 actuator to sustain the centrifugal loads it would have to cope with when installed on the future rotor model. The actuator, equipped with a dummy flap, mocking realistic mass and inertia, was installed inside an aluminum frame, closed by trap doors, in order to avoid any aerodynamic influence. Figure 4 presents the internal arrangement of the centrifugal model.

Several sensors were installed to record various data in operations :

- an inductive sensor (Keyence) and an associated oblique wedge ; the latter was necessary to allow measurement of the flap rotation since the measuring axis of the sensor was installed parallel to the rotation axis of the flap and pointing at one end of the flap ;
- a strain gauge bridge on lever blade ;
- a strain gauge bridge on the actuator elliptical frame ;
- a temperature probe on the lever blade to evaluate any possible thermal perturbation of the strain gauge bridges;
- a thermal gauge to monitor the possible heating of the system in the closed blade section ;
- an inert strain gauge along with an inert unsteady pressure sensor to assess any measurement perturbation due to actuator power lines.

The whole model was then mounted atop the BRAVoS rig to be tested.

BRAVoS rig

The BRAVoS (**B**anc **R**otor **A**dapté au **Vo**l **S**tationnaire) test rig is a helicopter rotor hover stand, which was designed and built at ONERA at the beginning of the 90's to :

- study the dynamic behavior, mainly with respect to stability, of various helicopter hubs (articulated, HMR, BMR) and various types of blades ;
- prepare wind-tunnel tests of such rotor hubs and blades in forward flight ;

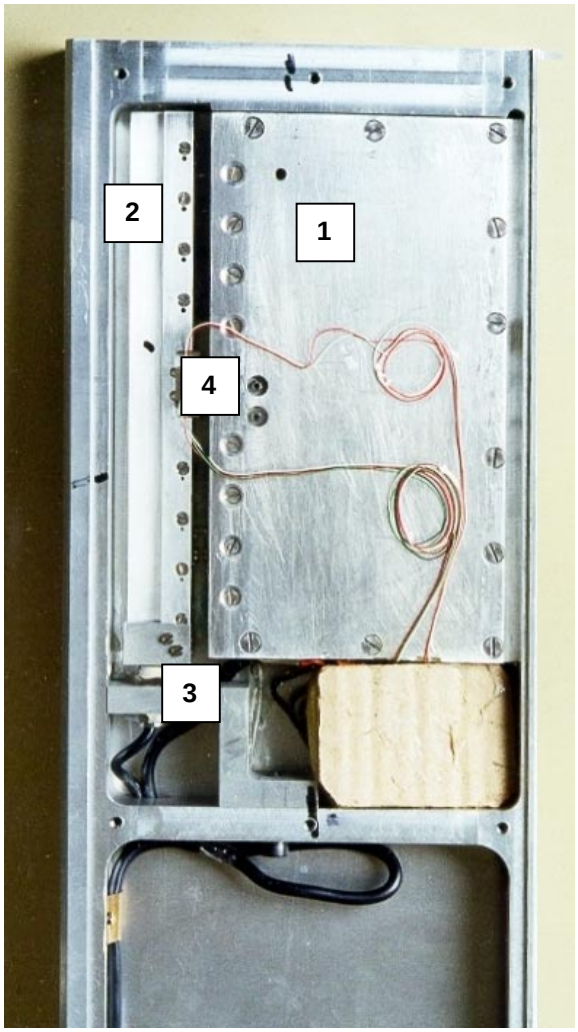

Figure 4 – Top view of the centrifugal model featuring : actuator (1), dummy flap (2), Keyence sensor (3), gauges on lever blade (4)

- establish transfer functions of rotor hubs [12] ;

- provide a spin test capability for innovative concepts such as active flaps or active twist.

Figure 5 shows the BRAVoS rig with a BMR hub and conventional cyclic swash-plate. The diameter of the rotor is 2 meters and the maximum achievable rotation speed is 3000 rpm. The rotor shaft is fitted with a power supply slip-ring and an additional telemetry system allows to record up to 64 channels.

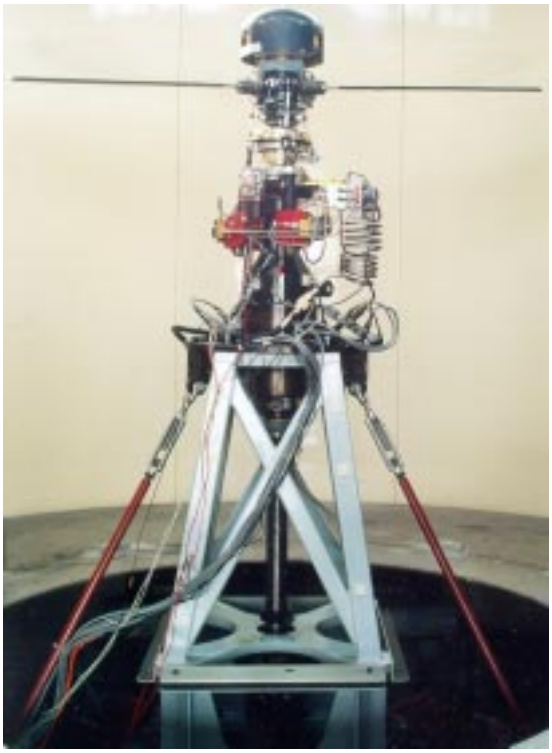

Figure 5 – BRAVoS hover test rig

Test program

As mentioned above, the rotating tests on the BRAVoS rig were devoted to the assessment of the behavior of the active flap system under realistic centrifugal loads. Consequently, the conditions of the tests were based on the planned operation conditions in both S1MA and DNW. As such, the maximum rotation speed of the future rotor, 115 rad/s, and the extreme spanwise position of the actuator were taken into account. Despite the smaller diameter of the BRAVoS rig and thanks to the high possible rotation speed (up to 3000 rpm), these configurations could be easily tested. The test program featured both quasi-steady flap deflections (1 Hz) and dynamic deflections up to 80 Hz, this value representing the fifth harmonic of the nominal rotation speed in S1MA and DNW wind tunnels. Several rotation runs were performed, either increasing or decreasing rotation speed. Deflections without rotation were checked after each run.

Characteristic results

Figures 6 and 7 show the flap deflection versus the amplifier voltage at different actuation frequencies, respectively under 0 g and 2000 g. The dynamic voltage was limited to ± 55 V because of the amplifier current limitation (up to 1 A).

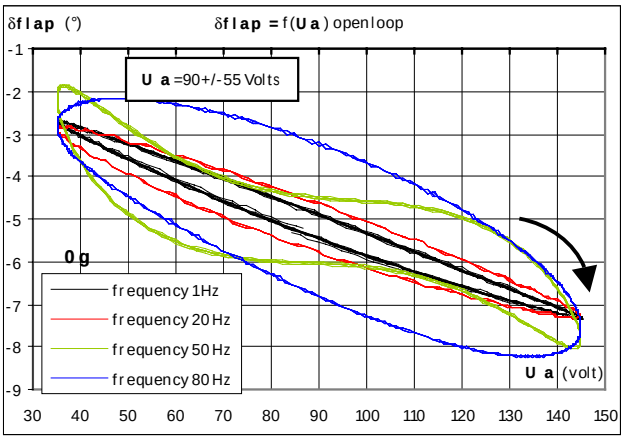

Figure 6 – Active flap system under 0 g

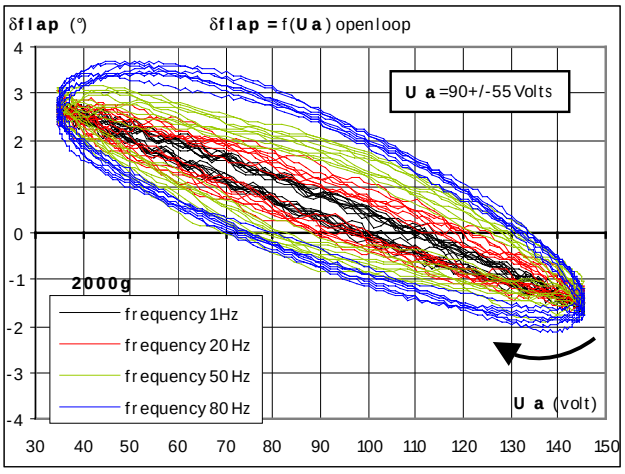

Figure 7 – Active flap system under 2000 g

At 0 g and 50 Hz, the waviness that can be noticed on the response curves was traced to be due to a subharmonic of the system first natural frequency (150 Hz). This was confirmed by the fact that this phenomenon could be avoided by adding a small dummy mass on the flap (and hence changing the natural frequency). However, the test campaign was performed without this dummy mass.

For each actuation frequency and various levels of centrifugal force, data were recorded during several upward and downward motion loops of the flap. A good repeatability of the measurements can be ob-

served on figure 7 although the system is submitted to high centrifugal loads. It must be underlined that the centrifugal tests were performed using only open-loop control of the actuator. Adding the closed-loop governor will of course improve the behavior of the system. Anyhow, the stroke loss between 0 g and 2000 g configurations was limited to around 10 % with this prototype, which is very encouraging. The discrepancies on the static values on figures 6 and 7 was due to a slight displacement of both the hinge blades and the elliptic frame surrounding the piezo stacks under the centrifugal loads, which induced a static deflection of the flap. After the tests, the model was dismantled part by part to assess any wear due to the centrifugal loads. It could then be seen that the fitting of the hinge blades in the surrounding rectangular frame was not perfect and a new clamping solution, based on centering pins, was then designed and used for subsequent testing steps. Similarly, the clamping of the elliptic frame on the external frame was reinforced.

Another specific feature of the model was that the actuator was not installed centered on the radial axis of the rotor in the closed frame. This means that a static component of lead-lag offset was simulated and experimental demonstration could thus be made that the active flap system could cope with such a configuration.

The analysis of the response of the thermal gauge located inside the model showed that no significant increase of inner temperature was measured. This confirmed laboratory thermal camera shots of the actuator, which showed that limited heat radiation could be observed and was moreover restricted to the piezo stacks. This is of prime importance since the future blade will be made of composite and any particular heat increase should thus be avoided.

Finally, the signals recorded from the inert strain gauge and pressure sensor presented no perturbation due to the voltage and current driving the actuator.

Conclusions and improvements

The centrifugal tests of a prototype of the active flap system were performed in the conditions of future wind tunnel tests and demonstrated the satisfactory behavior of the device.

Some minor changes in the mechanical installation of the actuator were estimated to be required and designed for the next qualification model.

AERODYNAMIC QUALIFICATION

New APA actuator

As already mentioned, the design and qualification of the flap active system were carried out in parallel with numerical simulations. Initially, the APA 230 actuator was selected with respect to industry specifications down-scaled to wind tunnel scale, along with the hypothesis that two actuators would be used in parallel. The results of the simulations and the availability of a new generation of actuators allowed to establish that the characteristics of a dual APA230 actuator configuration were in fact oversized with respect to the actual requirements for the future rotor blade model. Figure 8 shows the capabilities of one APA230 actuator in terms of stroke and blocking force plotted along with calculated values necessary to achieve significant acoustic and dynamic gains.

Another actuator, the APA500, featuring the same baseline architecture but with more favorable characteristics (see figure 8), could thus be selected. Additional assets of the APA500 were its lighter weight and smaller overall dimensions when compared to the previously chosen APA230, thus easing its integration in the blade.

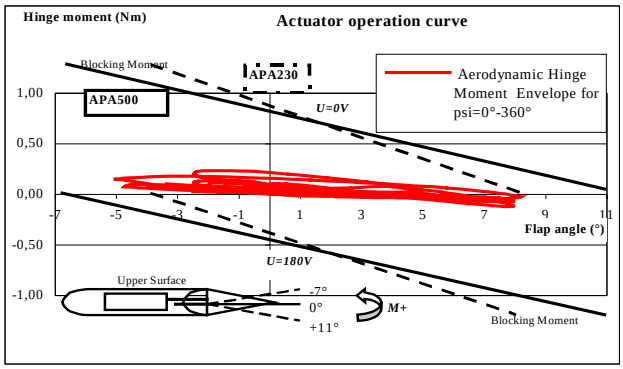

Figure 8 – Comparison between performance of two actuators and numerical requirements.

As a result, the assessment of the behavior of the active system under aerodynamic loads was performed using the APA500.

Test model

A specific model of a 2D-blade section incorporating the whole active system, i.e. actuator, lever blade, hinge blade and flap, was designed and manufactured, airfoil and flap being made of machined aluminum. The chord (140mm) and the airfoil (OA312) used on this model exactly match those of the future rotor blade model. Moreover, as the actuator on the future blade model will not be centered with respect to the flap span, due to the requirement of testing three spanwise flap positions along with available room allowing only two positions of the driving actuator, a similar configuration was used on the 2D model as it

might result in differential deflections between the two flap ends. Figure 9 shows the principle of the implementation of the active flap system inside the 2D model.

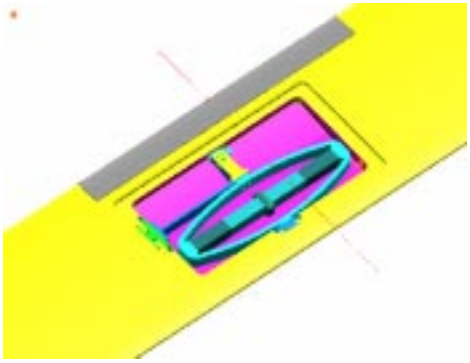

Figure 9 – Implementation of the active system in 2D-blade section

In order to allow steady and unsteady pitching movements of the whole model during wind tunnel tests, a rotating hydraulic jack was connected to the left-hand side of the model as illustrated on figure 10. A fixture featuring a ball-bearing supported the right-hand side of the model.

Figure 10 – Hydraulic rotating jack

The instrumentation of the model consisted in :

- a strain gauge bridge on the elliptic frame to monitor the actuator operations ;
- a strain gauge bridge on the lever blade ;
- a strain gauge bridge on a thinner measuring blade parallel to the lever blade. It was feared that the high stress level in the lever blade might cause the bridge installed on it to fail, which effectively occurred ;
- two Hall effect sensors respectively located at each end of the flap ;
- an inert strain gauge and an inert unsteady pressure sensor to assess once again the possible influence of the driving voltage and current of the actuator on such sensors, as the future blade model will be heavily instrumented ;
- a rotating potentiometer mounted on the hydraulic jack to provide accurate control of the angle of attack of the whole model.

S3MA wind-tunnel

The tests under aerodynamic loads of the active system were carried out in the S3MA blow-down wind tunnel located at ONERA Modane facility. This wind tunnel had been previously used within the frame of the RPA project to evaluate the aerodynamic efficiency of an OA312 airfoil equipped with flaps of both initial concepts (servo-flap and direct lift flap). A transonic 800x560-mm test section was used, featuring perforated floor and ceiling along with plain walls. As the behavior of the active system was the primary objective of the test campaign, no detailed aerodynamic measurement was required from the wind-tunnel team.

Flap deflection control strategy

Initially, it had been decided to rely on the signals streaming from strain gauges implemented on either the lever blade or the parallel measuring blade to achieve the control of the flap deflection. However, laboratory calibration tests performed prior to S3MA tests demonstrated that this option was not the optimal one since :

- the stiffness of the hinge blade was not taken into account by the controller and the resulting equivalent combined mechanical/electronic stiffness of the system was not high enough ;
- the natural torsion of the flap under load was not taken into account. This point could be of importance since the lever blade is not centered with respect to flap span.

Consequently, it was decided to use the signals coming from the Hall effect sensors located at both ends of the flap to control the flap deflections. A filter with a cutting frequency of 100 Hz was used to get rid of the modal frequencies of the flap system.

Test program

The test program was chosen to simulate the various aerodynamic conditions that the active system will encounter during the future rotor tests in both S1MA and DNW wind tunnels. Deriving from numerical simulations performed by various ONERA Departments (Applied Aerodynamics, Acoustics, Structural Dynamics), characteristic Mach number / airfoil angle of attack configurations were selected, typical of ad-

vancing, retreating and fore/aft blade azimuthal positions. Both the steady and unsteady behavior of the model was tested during the following configurations :

- flap deflections with airfoil fixed ;
- airfoil oscillations with flap fixed at 0° ;
- combined flap/airfoil oscillations.

The baseline airfoil oscillation frequency was set at 16 Hz, typical of the nominal rotation speed of the future rotor. According to simulations, flap frequencies extending till 5-per-rev (80 Hz) were documented. A quasi-steady (0.5 Hz) approach was used to assess the steady behavior of the active system, to both get rid of any possible mechanical play and exhibit any hysteresis phenomenon. In any configuration, the main objectives of the tests were to record the maximum achievable flap amplitude and the associated control characteristics.

Calibrations

Prior to the tests in S3MA wind tunnel, comprehensive laboratory tests were performed on the model to ensure that the system would behave the way it was designed to. Two main points were focused on :

- the calibration procedure of both Hall effect sensors at flap ends and strain gauge bridges ;
- the assessment of the influence of the dynamic actuation of the whole model on the flap itself.

Sensors calibration. Concerning the calibration of the Hall effect sensors and strain gauge bridges, a dual method was used, with the help of laser telemeters and vibrometers. As the chord of the flap is rather small (21 mm) and in order to increase the precision of the calibration phase, a special extension was designed, which could be clipped on the trailing edge of the flap (see figure 11). In parallel, a special mounting frame was manufactured, which could be installed on the airfoil model. Two Keyence laser telemeters were located on the special mounting, pointing at the upper surface of the extension, covered with white paint. As the distance between the two telemeters was perfectly known, as well as their chordwise position with respect to the equivalent flap hinge axis, the measurement of the two distances to the extension allowed to calculate the actual flap deflection with a very good accuracy. The simultaneous recording of the signals coming from the Hall effect sensors and strain gauges led to the calibration of these sensors. However, due to the mass of the extension compared to the mass of the flap, the natural frequencies of the latter were tremendously reduced and this induced some instabilities in the control system, well below the planned maximum experimental flap actuation frequency. Consequently, only static and pseudo-static (0.5 Hz) calibrations could be performed.

In order to check that the calibration curves were not affected by the various actuation frequencies, a laser vibrometer was also used during the pseudo-static calibrations, aiming at reflective patches temporarily glued on the flap. Once the extension was dismounted, the flap could be actuated at the various planned frequencies and the relevant Hall effect sensors and strain gauges signals recorded to check the calibration parameters. No specific correction was estimated necessary.

Once the model mounted in the wind tunnel, the calibration was done once again for final checks right before the blow-downs as illustrated on figure 11.

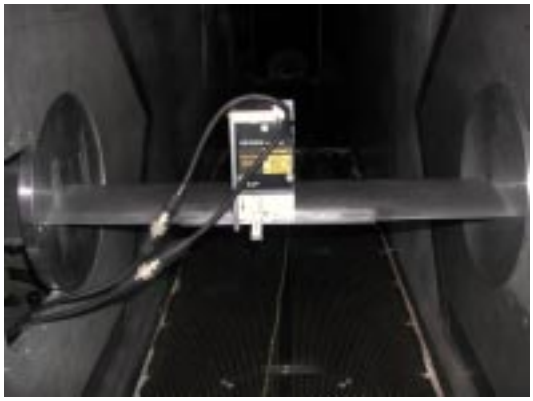

Figure 11 – Calibration device on the model in the S3MA wind tunnel

Influence of model pitching. According to the test program, some isolated airfoil oscillations and combined flap/airfoil oscillations were planned. It was mandatory to check that the movement of the whole model (inertia effect for example) did not affect the flap behavior. Therefore, relocatable accelerometers were temporarily glued on the trailing edges of both the airfoil and the flap (see figure 12), the latter being held at a constant deflection angle by the control system (closed loop configuration).

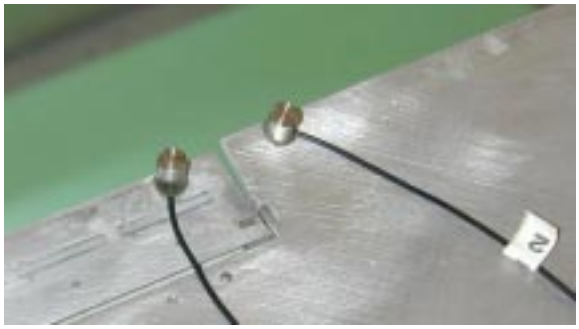

Figure 12 – Accelerometers on airfoil and flap (at rest)

The airfoil was then oscillated at 16 Hz, typical of future rotor blades cyclic pitch excursions. No difference between the acceleration levels given by the sensors either glued on the airfoil or on the flap could be noticed thus demonstrating that the flap inertia had no detectable influence given the existing lever blade stiffness (irreversibility of the system).

Characteristic results

As exposed above, the test program included several Mach numbers (0.3, 0.45, 0.65, 0.8) and corresponding airfoil angles of attack (both static and dynamic values). In order to prevent any mechanical problem on the flap system due to high aerodynamic loads, the speed of the blow-downs was gradually increased, three typical oscillation configurations being performed at each speed step. A significant amount of data was accordingly recorded, the detailed analysis of which is still under examination. The results presented here are essentially related to the pseudo-static actuation of the flap for fixed airfoil angles of attack.

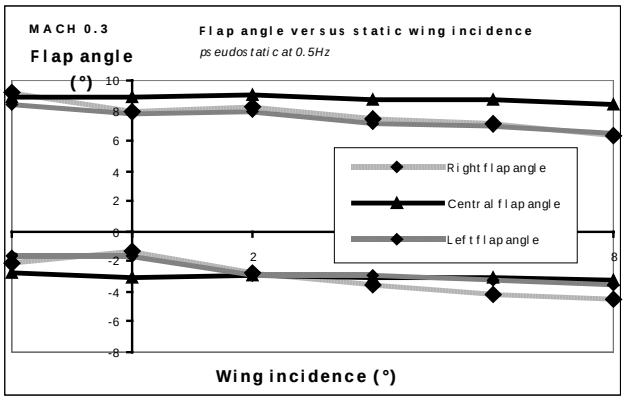

Figure 13 – Flap deflections at Mach=0.3

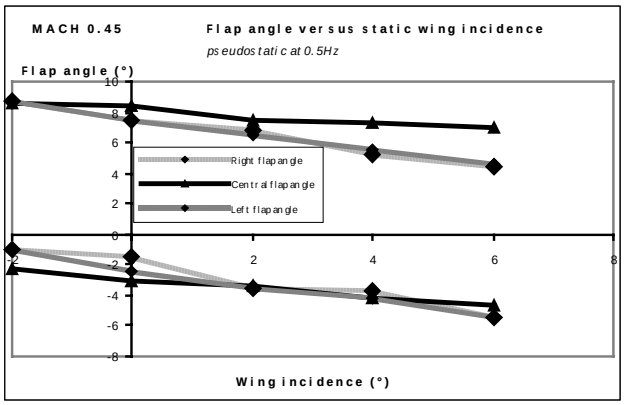

Figure 14 – Flap deflections at Mach=0.45

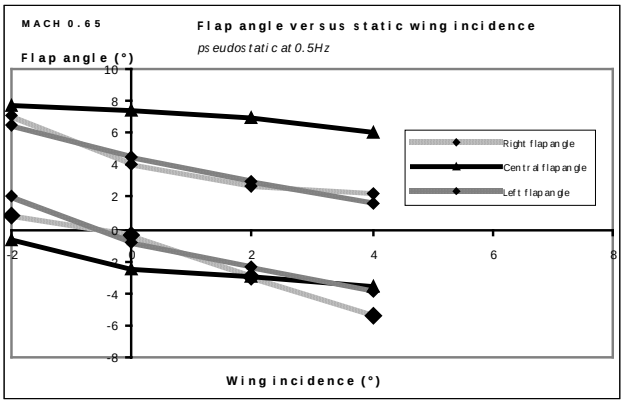

Figure 15 – Flap deflections at Mach=0.65

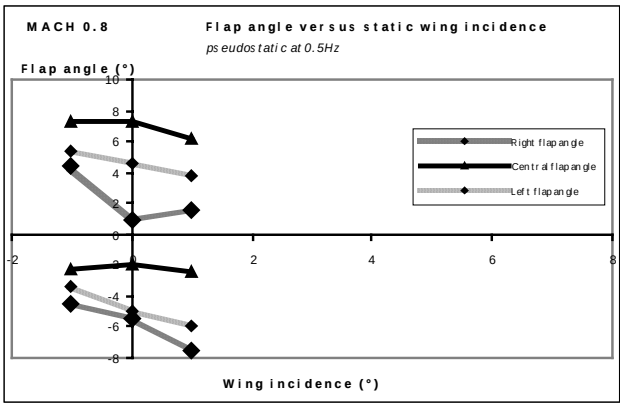

Figure 16 – Flap deflections at Mach=0.8

Figures 13 to 16 show the measured flap deflections (maximum upward and downward values) at three different locations, i.e. lever blade (central flap angle), left and right flap ends, with respect to airfoil angle of attack for the 4 explored Mach numbers.

The following comments can be made :

- at low Mach numbers (0.3 and 0.45), a fairly good agreement can be seen between the three flap deflection measurements for the downward position, although some discrepancies start to appear for high values of airfoil angle of attack ;
- at these Mach numbers, similar values are given by both Hall effect sensors for upward flap deflection, but discrepancies with the value measured at the lever location can be noticed ;
- at Mach=0.65, the discrepancies between lever blade and flap ends measurements increase, as well as the difference between deflection of both flap ends when compared with lower Mach numbers ;
- at Mach=0.8, significant discrepancies between right and left flap ends, as well as between Hall effect sensors and lever blade gauges are observed.

Deriving from these comments, it can be said that the behavior of the flap system under aerodynamic loads is satisfactory at low wind speeds. When the airstream speed is increased, discrepancies increase between the deflections at both flap ends and the flap driving point. Moreover, for the highest Mach number, significant discrepancies are noticed between flap ends. All these information tend to prove that the intrinsic stiffness of the flap is not high enough and that the flap is distorted (in both torsion and flexion) under high aerodynamic loads. The consequence will be that the flaps for the rotor will have to be made of carefully laid-up carbon plies.

Concerning the dynamic actuation of the flap (frequency equal or above 16 Hz), figures 17 and 18 present another typical effect noticed during the tests.

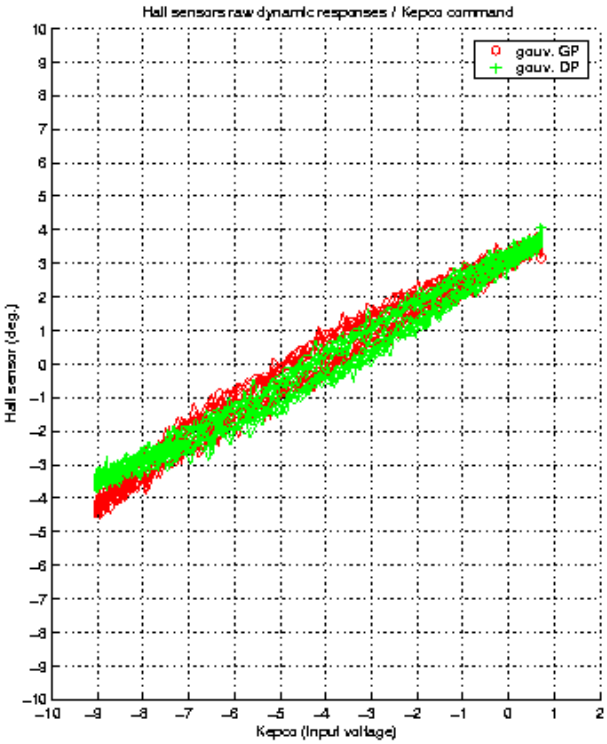

Figure 17 – Flap deflection vs. amplifier command voltage at Mach=0.3

As the airstream speed was increased, the slope of the flap deflection with respect to the power supply became inverted. At first, during the test campaign, an aerodynamic effect such as flap suction was suspected. Additional following laboratory tests, made by clamping the trailing edge of the flap to the trailing edge of the airfoil and powering the actuator, allowed to demonstrate that the hinge blades could deform, resulting in the chordwise displacement of the pseudo-axis of the flap. A side effect of such a phenomenon was that the equivalent flap rotation axis moved towards the measurement axis of the Hall effect sensors, resulting in significantly reduced amplitudes of associated signals, rendering the control of the flap almost impossible. Once this situation thoroughly analyzed, a fixing solution was designed in the form of pseudo-knee joints implemented at both ends of the flap. This new design allows to prescribe the flap rotation axis, without facing problems of wear. Consequently the closed-loop control of the flap under aerodynamic loads should be tremendously eased.

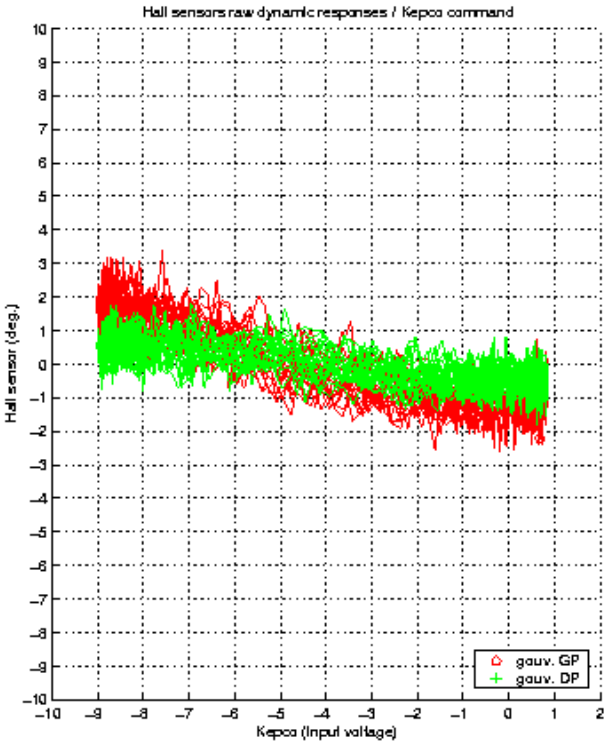

Figure 18 - Flap deflection vs. amplifier command voltage at Mach=0.65

Conclusions and improvements

An active flap system was tested under realistic aerodynamic loads without any mechanical breakdown, demonstrating the robustness of the design.

A good behavior of the system could be obtained at low Mach numbers, but some problems arose for higher speeds. Careful data analysis and additional laboratory tests allowed to identify the reasons of these setbacks and subsequent solutions could be proposed.

A new test campaign under centrifugal loads, to fully clear the system featuring the APA 500 actuator, along with the pseudo-knee joints, and taking into account the coning effect of the future rotor was then performed. The first analysis of the corresponding results showed that the stroke loss under 2300 g could

now be kept under 8 %, which proves that the improvements are worthwhile.

CONCLUSION

A project called RPA (Rotor à Pales Actives) was launched to study the influence of active trailing edge flaps on both the acoustic and dynamic characteristics of a full-scale helicopter main rotor. Once an optimal flap configuration numerically defined, the design of a wind-tunnel scale rotor model was started to validate the calculations.

The actuation of the flaps on the rotor model will be achieved by relying on an innovative active flap system, based on a piezo-electric actuator, the APA design, from the French CEDRAT Company.

To clear the active system for use on the rotor model, two elementary models (centrifugal and aerodynamic) were designed, manufactured and tested to assess the behavior of the trailing edge flap active system. Even if minor modifications are required on the system, the centrifugal aspects were easily mastered. The behavior under aerodynamic loads was not straightforward to assess, especially at high speeds. However, improvements are already designed and will be implemented in the future rotor model.

The feasibility of such an active flap system at wind-tunnel scale is thus considered as demonstrated.

FUTURE APPLICATIONS

Given the satisfactory results obtained with the APA 500 and APA 230 actuators, developments are now under way to improve these actuators by designing an elliptic frame made of composite to obtain a lighter actuator. Additionally, research tasks aiming at up-scaling the active flap system for full-scale helicopters are presently being addressed.

ACKNOWLEDGMENTS

The authors would like to thank the French Civil Aviation Authorities, Ministry of Defense and Eurocopter for supporting the RPA project as well as the manufacture department (ONERA/DGMT/DERM) and the S3MA test team for their commitment to the tests.

REFERENCES

1. **Meeting Paper** - Reneaux J., Thibert J.J., “The Use of Numerical Optimization for Airfoil Design”, AIAA 3rd Applied Aerodynamics Conference, Colorado Springs, Colorado (USA), October 1985
2. **Meeting Paper** - Bezard H., “Rotor Blade Airfoil Design by Numerical Optimization and Unsteady Calculations”, 48th AHS Forum, Washington DC, June 1992
3. **Meeting Paper** - Lim J.W., Chopra I., “Aeroelastic Optimization of a Helicopter Blade”, 44th AHS Forum, Washington DC, June 1988
4. **Periodical** - Adelman H.M., Mantay W.R., Walsh J.L., Pritchard J.J., “ Integrated Multidisciplinary Rotorcraft Optimization Research at the NASA Langley Research Center”, Vertiflite, March-April 1992, Vol. 38, N°2
5. **Meeting Paper** - Leconte P., Geoffroy P., “Dynamic Optimization of a Rotor Blade”, AHS Aeromechanics Specialists Conference, San Francisco, 1994
6. **Meeting Paper** – Delrieux Y. and al, “The ONERA-DLR Aeroacoustic Rotor Optimization Program ERATO : Methodology and Achievements”, AHS Aerodynamics, Acoustics and Test and Evaluation Technical Specialists Meeting, San Francisco, California, January 23-25, 2002
7. **Meeting Paper** - Kube R. and al, “ HHC Aeroacoustic Rotor Tests in the German Dutch Wind-Tunnel : Improving Physical Understanding and Prediction Codes”, 52nd AHS Forum, Washington DC, June 4-6 1996
8. **Meeting Paper** - Leconte P., Kube R., “ Main Rotor Active Flaps : Numerical Assessment of Noise and Vibration Reduction”, 2nd DLR-ONERA Aerospace Symposium, Berlin (Germany), June 15-16, 2000
9. **Meeting Paper** - Leconte P., Rapin M., Van der Wall B., “ Main Rotor Active Flaps : Numerical Assessment of Vibration Reduction”, 57th AHS Annual Forum, Washington (USA), May 09-11, 2001
10. **Meeting Paper** - Toulmay F., Kloeppel V., Lorin F., Enenkl B., Gaffiero J., “ Active Blade Flaps – The Needs and Current Capabilities”, 57th AHS Annual Forum, Washington (USA), May 09-11, 2001
11. **Meeting Paper** – Chopra I., “Status of Application of Smart Structures Technology to Rotorcraft Systems”, presented at Innovation in Rotorcraft Technology, Royal Aeronautical Society, London (UK), 25-26 June, 1997
12. **Meeting Paper** – Costes J.J., “Large band-with identification of a rotor model”, 27th European Rotorcraft Forum, Moscow (Russia), 11-14 September, 2001